available at www.sciencedirect.com

ScienceDirect

journal homepage: www.elsevier.com/locate/modo

MECHANISMS OF DEVELOPMENT

Drosophila Axud1 is involved in the control of proliferation and displays pro-apoptotic activity

Alvaro Glavic[a,*], *Cristina Molnar*[b], *Darko Cotoras*[a], *José F. de Celis*[b]

[a]*Millennium Nucleus Center for Genomics of the Cell, Department of Biology, Faculty of Sciences, University of Chile, Las Palmeras 3425, Santiago, Chile*

[b]*Centro de Biología Molecular "Severo Ochoa" CSIC-UAM, Cantoblanco 28049, Madrid, Spain*

ARTICLE INFO

Article history:
Received 17 March 2008
Received in revised form
18 November 2008
Accepted 19 November 2008
Available online 28 November 2008

Keywords:
AXUD1 tumour suppressor
Cell cycle control
Apoptosis

ABSTRACT

Cell division rates and apoptosis sculpt the growing organs, and its regulation implements the developmental programmes that define organ size and shape. The balance between oncogenes and tumour suppressors modulate the cell cycle and the apoptotic machinery to achieve this goal, promoting and restricting proliferation or, in certain conditions, inducing the apoptotic programme. Analysis of human cancer cells with mutation in *AXIN* gene has uncovered the potential function of AXUD1 as a tumour suppressor. It has been described that Human AXUD1 is a nuclear protein. We find that a DAxud1-GFP fusion protein is localised to the nucleus during interphase, where it accumulates associated to the nuclear envelope, but becomes distributed in a diffused pattern in the nucleus of mitotic cells. We have analysed the function of the *Drosophila* AXUD1 homologue, and find that *DAxud1* behaves as a tumour suppressor that regulates the proliferation rhythm of imaginal cells. Knocking down the activity of *DAxud1* enhances the proliferation of these cells, causing in addition a reduction in cell size. Conversely, the increase in *DAxud1* expression impedes cell cycle progression at mitosis through disturbance of Cdk1 activity, and induces the apoptosis of these cells in a JNK-dependent manner.

1. Introduction

Proliferation and apoptosis are the principal contributors to the establishment of organs and organisms' size and shape (reviewed in Leevers and McNeill, 2005). Both processes are genetically controlled, being proliferation rhythms and events of morphogenetic apoptosis a key component of animal development. Besides the basic cyclin-based machinery, an increasing number of signalling pathways and regulatory proteins, like proto-oncogenes and tumour suppressors, have been described to modify the cell cycle, often operating at the G1/S or G2/M transitions (Lee and Orr-Weaver, 2003). In *Drosophila*, the Cdk2/Cyclin E complex is one important element controlling the G1/S transition (Knoblich et al., 1994; Secombe et al., 1998; Duronio et al., 1998). Other proteins such as the E2F/Dp heterodimer, Myc, Ras and several other signalling pathways modify the levels of Cyclin E, consequently changing the rate of the G1/S transition (Royzman et al., 1997; Prober and Edgar, 2000; Wu et al., 2003; Bhat and Apsel, 2004; Oskarsson et al., 2006). The Cdk1/Cyclin B complex ultimately modulates the G2/M transition. Cdk1 is regulated by an elaborated arrangement of phosphorylation and dephosphorylation events, and in turn, controls the activity of Cdk1/Cyclin B complexes. The Cdc25/String phosphatase is one of the best-characterised activators of Cdk1 activity, and Tribbles, Wee1 and Myt1 kinases regulate protein levels and its phosphatase activity (Mata et al., 2000; Price et al., 2000; Price et al., 2002). In addition to G1/S and G2/M restrains, a

* *Corresponding author.* Tel.: +56 2 9787179; fax: +56 2 2763802.
E-mail address: alglavic@uchile.cl (A. Glavic).
0925-4773/$ - see front matter
doi:10.1016/j.mod.2008.11.005

third control point exists in the M/G1 transition. Spindle checkpoint proteins, anaphase promoting complex and Cdk1 are some of the elements that limit the rate of mitosis progression and subsequent re-enter into G1 phase (Weigmann et al., 1997; Margottin-Goguet et al., 2003; Vidwans et al., 2003; Stumpff et al., 2005; Muller et al., 2006; Buffin et al., 2007; Sumara et al., 2004; Leismann and Lehner, 2003; Huang and Raff, 1999). Tumour suppressors participate at the control points by imposing rate-limiting inputs, and mutations in these proteins in pathological conditions or in experimental situations where their levels are augmented, promote unrestrained proliferation or lead to cell death (Pellock et al., 2007; Hamaratoglu et al., 2006; Wu et al., 2003; Ae et al., 2002; Ollmann et al., 2000; Huang et al., 1999).

The uncontrolled activation of canonical Wnt pathway has been described in a variety of cancers and tumour cell lines and thus elements that reduce Wnt signalling have been described to have tumour suppressor activity. Axin is one of the negative components of this pathway and mutations on it have been associated with cancer cells (reviewed by Huang and He, 2008). Recently, analysing the transcription profile of human cancer cells with mutations in the *AXIN* gene, Ishiguro et al. described a transcript that is under-represented in cancer cells compared with normal cells (Ishiguro et al., 2001). *AXIN* expression was able to induce its transcription in a LEF/TCF independent mode, and as a result, they named this putative tumour suppressor gene *AXUD1* (Axin Upregulated 1). Later, Gingras et al. analysed the *in vivo* function of the three mouse paralogs (CSRNP-1, -2 and -3) by generating the corresponding knockout animals, but they could not find evidence of a role for these genes as tumour suppressors (Gingras et al., 2007). There is a single orthologue of the AXUD1/CSRNP family in *Drosophila* that maintains the structural features described for AXUD1 and CSRNPs proteins, which we named *DAxud1*. We investigated the function of *DAxud1* using the genetic and molecular advantages of the fly model, aiming to analyse its potential activity as a tumour suppressor. Our results indicate that DAxud1 is a nuclear protein that antagonises proliferation during mitosis in a Cdk1-dependent manner. DAxud1 reduction confers cells with a proliferation advantage that leads in the adult wing to higher cell densities accompanied by a reduction in cell size. Conversely, over-expression of *DAxud1* blocks mitosis and promotes apoptosis through the activation of the JNK pathway.

2. Material and methods

2.1. *Drosophila melanogaster* strains and phenotypic analysis

The P-GS insertion *c-676* was isolated in a mutagenesis screen designed to identify genes affecting vein differentiation, and it is localised in the 5′ UTR of CG4272 (Molnar et al., 2006). We used the following *Drosophila* UAS lines: *UAS-puc2A*, *UAS-p35*, *UAS-Dronc*^{DN}, *UAS-Cdk1-myc*, *UAS-Stg*, *UAS-Cdk2-myc*, *UAS-E2F/Dp*, *UAS-Dicer* and *UAS-CD8::GFP*. We also used the following Gal4 lines: *ey-Gal4*, *sal*^{EPv}*-Gal4* (*sal-Gal4*; C. Cruz and JFdC, unpublished), *GMR-Gal4*, *638-Gal4* and *UAS-GFP*, *hh-Gal4/TM6b* and the reporter lines *dad-lacZ* and *brk-lacZ*. The *sal-Gal4, UAS-DAxud1* stock was made by meiotic recombination. JNK pathway activation was assayed using the *puc*^{E69} enhancer trap line (Martin-Blanco et al., 1998). All stocks not described in the text can be found in Flybase (http://www.flybase.org). All phenotypes were analysed at 25 °C unless otherwise stated, and wings were mounted for microscopic examination in lactic acid-ethanol (1:1). Pictures were taken in an Axiophot microscope with a Spot digital camera and processed using Adobe Photoshop. Areas were quantified with the Photoshop histogram tool.

2.2. *Generation of UAS-DAxud1, UAS-DAxud1-GFP and UAS-DAxud1-iRNA constructs*

UAS-DAxud1 was constructed cloning the complete RE38563 insert into the pUAS-T vector using KpnI and NotI restriction enzymes. The DAxud1-GFP fusion protein was generated cloning the PCR fragment amplified with the forward and reverse primers: 5′- GGGGAATTCCGCAAATTGCA AAAAGGATAA-3′ and 5′- GGGCCGCGGGGAGGACTCGCTTGTC GCTGG-3′ using the GH09817 clone as template. This fragment was cloned into the pEGFP-N1 vector (Clontech) digested with the EcoRI and SacII restriction enzymes (underlined in the primers) and later subcloned in the pUAS-T vector using the EcoRI and NotI sites. The *DAxud1* fragment (473 bp) employed to produce the *UAS-DAxud1-iRNA* construct was amplified from the RE38563 clone using the primers: forward 5′-CAT GTTGCAGGGGTCCAGCG-3′ and reverse 5′-GTGTCCGCCGG GCCGTGAGC-3′. The PCR product was cloned into the pST Blue vector (Novagene) and sequenced. Next, it was subcloned using the SacI and BamHI sites in the pHIBS vector (Nagel et al., 2002). The NotI PstI fragment from pST Blue *DAxud1* and the PstI XhoI fragment from pHIBS *DAxud1* were directionally cloned in pBK SK using the NotI and XhoI sites to obtain the 473 bp DNA hairpin construct. Finally, the *DAxud1-iRNA* construct was introduced in the pUAS-T vector using the KpnI and NotI sites. A standard germ cell transformation protocol was followed to obtain at least three transgenic lines for each construct (Spradling and Rubin, 1982).

2.3. *Inmunofluorescence and in situ hybridization*

Mouse monoclonals anti-Arm (1/100), anti-Osa (1/50), anti-Elav (1/20), anti-Dlg (1/100), anti-Dlg (1/200), anti-FasIII (1/100), anti-Wg (1/100) and anti-BrdU (1/100) (Hybridoma bank), rat anti-Sal (dilution 1/200; Barrio et al., 1999), anti-Dll (1/250; Vachon et al., 1992 and rabbit anti-PH3 (dilution 1/500, Upstate), anti-Myc (1/100, Santa Cruz), anti-ßGal (dilution 1/200, Cappel) and anti-activated Caspase 3 (1/100, Cell Signalling) were employed. We also used rabbit anti-Nup214, a gift of Christos Samakovlis (1/200). Secondary antibodies were from Jackson Immunological Laboratories (used at 1/200 dilution) and nuclei were stained with Topro 3A (Invitrogen). Third instar imaginal discs were dissected, fixed and stained as described in de Celis (1997). Confocal images were captured using a Zeiss LSM 510 Meta microscope. In situ hybridization in imaginal discs and embryos was carried out as described in de Celis (1997) with minor modifications. Sense and anti-sense digoxigenin-labelled RNA probes were prepared with T3 and T7 RNA polymerase using the RE38563 clone as template.

2.4. RT-PCR analysis

Actin, *Cdc2* and *DAxud1* transcriptional profiles were analysed in third instar wing discs of control, *DAxud1* increased expression (*638-Gal4/UAS-DAxud1*) and *DAxud1* loss-of-function (*638-Gal4/UAS-iDAxud1*) conditions. Twenty wing discs of each genotype were dissected, total RNA extracted using Trizol reagent (Invitrogene) and cDNA synthesised using the Superscript II kit (Invitrogene) following manufacturer instructions. PCR analysis was performed using the following protocol: denaturation = 95 °C 5 min.; 25–30 cycles = 95 °C 45 s., 55 °C 1 min. and 72 °C 40 s.; final elongation = 72 °C 10 min. The following primers were used: *Actin* forward, 5′-GGCCGGACTCGT CGTACTCCTGC-3′ and reverse, 5′-GAGCAGGAGATGGC CACCG CTGC-3′; *Cdc2* forward, 5′-CGGGCCAA ATTGTGGCAATG A-3′ and reverse, 5′-AAAGGATCGGCCAA GTCCAAAG-3′; *DAxud1* forward, 5′-GCGAATTCCGATGCTATAG ATCTGGTCCC-3′ and reverse, 5′-GCTCTAGAAGGAAGTACGCG GATGTTGA-3′.

2.5. TUNEL and BrdU assays

BrdU incorporation was examined incubating wing and eye discs in 0.05 mM BrdU in PBS for 20–30 min at 25 or 29 °C. Tissues were fixed in modified Carnoy's solution (3:1 ethanol: lactic acid) for 2 min, washed in PBS four times for 10 min each and subsequently the DNA was hydrolysed with 2 M HCl for 20 min. After four washes in PBS-0.1% Tween the discs were incubated with anti-BrdU antibody (1/100). TUNEL was carry out with the in vivo cell death detection kit (Roche) according to manufacturer instructions modifying the permeabilizing step by incubating in 0.3% Triton X100-0.1% sodium citrate solution for 30 min at 65 °C. Later washes and secondary antibody incubation was done following standard immunofluorescence protocols.

2.6. MARCM and Flip-out clonal analysis

MARCM clones: Flies of *y w hsFLP1.22; UAS-GFP FRT42D/CyO; UAS-iDAxud1* and *y w hsFLP1.22 TubGal4/FM7; TubGal80 FRT42D/CyO* genotypes were crossed, and the offspring subjected to heat shock treatments at 36 ± 12, 60 ± 12 or 84 ± 12 h after egg laying (AEL) for 1 h. Third instar wandering larvae were dissected, fixed and visualised in the confocal microscope. Clon (GFP positive) and twin areas were measured in isolated twin spots using the Photoshop histogram tool.

3. Results

The CG4272 gene is located in the left arm of chromosome 2 at cytological position 22E1. CG4272 produces 2 transcripts of 4126 (CG4272-RA) and 3782 (CG4272-RB) nucleotides encoding a single polypeptide of 852 amino acids (Gelbart et al., 1997). Protein blast using the blastp algorithm identifies a number of related sequences in both vertebrate and invertebrate organisms. The vertebrate homologues belong to the Axin-upregulated family (Axud), also named TGFβ-induced apoptotic proteins (TAIP). Conservation of *Drosophila* CG4272 and related invertebrate members range between 38% identity (*Aedes aegypti*) to 60% identity (*Anopheles ganbiae*). Identity between CG4272 sequence and its vertebrate counterparts is between 43% (*Danio rerio*) to 45% identity (*Homo sapiens* AXUD1). To analyse the conservation of the *Drosophila* CG4272 protein we performed a phylogenetic analysis with sequences recovered using the BLAST-PSI programme. The criterion to select the putative orthologues was the highest level of similarity between the human AXUD1 protein and one predicted coding sequences in each genome. Thus, vertebrate paralogues were excluded to simplify the phylogenetic tree (Fig. 1A). Protein sequence comparison using CLUSTALW and consensus tree analysis using the PAUP* programme in the neighbour joining algorithm configuration, shows that AXUD proteins in vertebrates are highly conserved (91–98% identity among mammalian orthologues), and that the main conserved domain with *Drosophila* and vertebrates is a central acidic domain of 88 amino acids (Fig. 1B). This domain is predicted to be a presumptive phospho-acceptor site for acidophilic serine/threonine kinases (ExPASy Tools – NetPhos 2.0 server; http://www.cbs.dtu.dk/services/NetPhos/, Blom et al., 1999).

In situ hibridization analysis shows that *DAxud1* is maternally contributed, and its transcripts localise homogenously in the early embryo and during the blastoderm stage (Fig. 1D and E). Later on, the expression is restricted to the cephalic furrow and mesodermal tissue along the anterior-posterior axis, as well as to the anterior and posterior gut precursors (Fig. 1F). Afterwards, *DAxud1* expression decreases from tissues that have completed morphogenetic movements, and continues mostly in posterior and anterior gut precursors as well as in muscle precursors (not shown). The expression of *DAxud1* is generalised in the wing blade of the wing disc (Fig. 1G) and in the proliferative domains of the eye disc anterior to the morphogenetic furrow (Fig. 1H and I). Note that no expression is detected in differentiating ommatidia (asterisk in Fig. 1H), and a clear reduction is observed posterior to the morphogenetic furrow, where the second mitotic wave occurs (arrowhead in Fig. 1I).

Human and mouse AXUD proteins localise in the cell nucleus (Ishiguro et al., 2001; Gingras et al., 2007). In fact, mice AXUD/TAIP paralogues cluster within a family of proteins with transcription factors characteristics (Gingras et al., 2007). Computational prediction (Proteome Analyst – Subcell Specialization Server 2.5 (http://pasub.cs.ualberta.ca:8080/pa/Subcellular) suggests that *Drosophila* Axud1 is also a nuclear protein (99.9%). To study DAxud1 sub-cellular localisation, we generated a *DAxud1-GFP* fusion protein and express it in the wing imaginal disc (Fig. 2). DAxud1-GFP is localised in the cell nucleus in imaginal cells (Fig. 2A, B). Interestingly, the level of DAxud1-GFP is consistently lower in mitotic cells, those appearing in the apical side of the epithelium, than in cells in other phases of the cell cycle (Fig. 2A, B and F). Staining of *sal-Gal4/UAS-DAxud1-GFP* discs with the nucleic acid marker Topro shows that in interphase cells DAxud1-GFP protein accumulation is higher in a region not labelled with Topro that might correspond to the inner nuclear envelope, and that DAxud1-GFP is excluded from the nucleolus (Fig. 2C–C″″). The accumulation of DAxud1-GFP in the inner nuclear membrane is also observed in salivary gland cells, where DAxud1-GFP

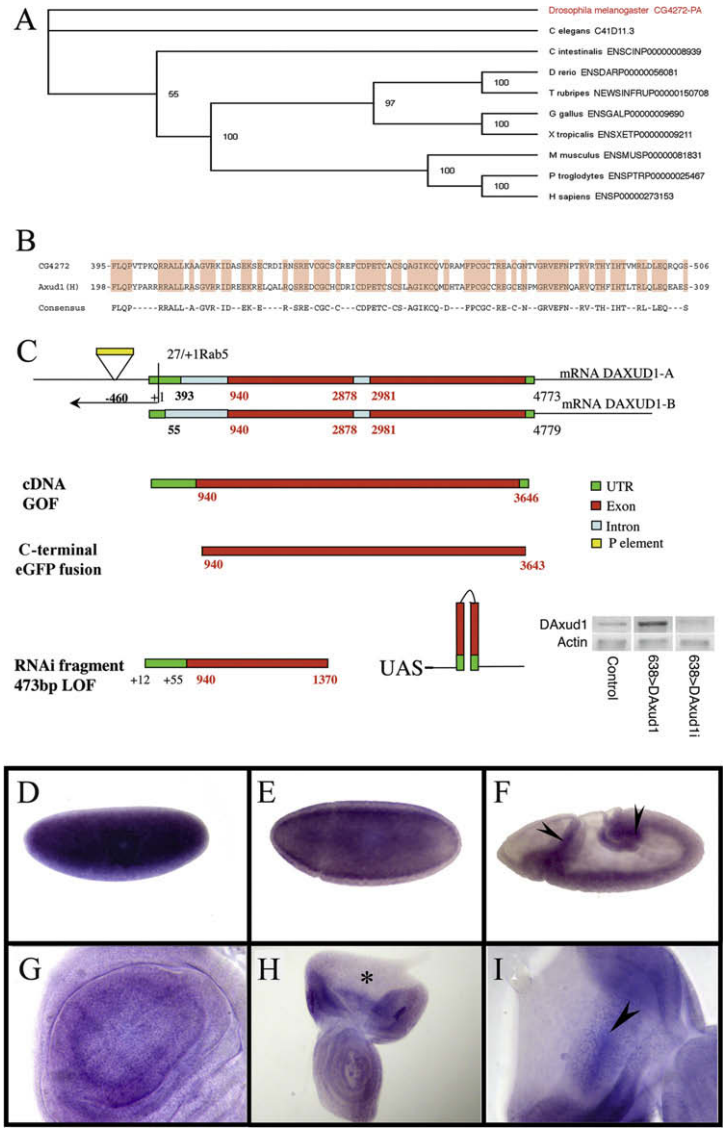

Fig. 1 – Expression and structure of CG4272 (DAxud1). (A) Bootstrap 50% majority-rule phylogram of AXUD1 proteins (1000 repetitions) generated with the PAUP* programme and neighbour joining algorithm. Sequence accession numbers: *C. elegans* C41D11.3; *C. intestinalis* ENSCINP00000008939; D. rerio ENSDARP00000056081; *D. melanogaster* CG4272-PA; *G. gallus* ENSGALP00000009690; *H .sapiens* ENSP00000273153; *M. musculus* ENSMUSP00000081831; *P. troglodytes* ENSPTRP00000025467; T. rubripes NEWSINFRUP00000150708; X. *tropicalis* ENSXETP00000009211. (B) Comparison of the 88 aa central acidic domain of AXUD and DAxud1. (C) Diagram of the *Drosophila* Axud1 locus, showing the predicted transcription start site and transcripts originated from it. Below is a scheme of UAS-DAxud1 (UAS-DAxud1), UAS-DAxud1-GFP fusion (UAS-DAxud1-GFP) and UAS-DAxud1 RNAi (UAS-iDAxud1) constructs, illustrating the coding regions (red) and DNA fragment employed in the RNA interference construct. To the right, a RT-PCR showing the variations in DAxud1 imaginal wing disc levels produced by the induction of the UAS-DAxud1 and UAS-iDAxud1 in the wing pouch in larvae of genotypes 638-Gal4, 638-Gal4/UAS-DAxud1 and 638-Gal4/UAS-iDAxud1. (D-H) Embryonic and imaginal DAxud1 expression. (D-F) DAxud1 RNA in situ hybridization at different stages during embryonic development, anterior to the left and dorsal up. (D) Stage 2 embryo, showing that DAxud1 is maternally contributed and its RNA located throughout the embryo. (E) At blastoderm stage, the DAxud1 mRNA is still ubiquitously distributed. (F) Expression of DAxud1 in the cephalic furrow (left arrowhead), anterior and posterior gut precursors (right arrowhead) and in the germ band, during germ band elongation. (G-I) DAxud1 in situ hybridization in third instar wing and eye imaginal discs. DAxud1 is expressed ubiquitously, yet with variable levels, in the wing imaginal disc (G). Expression is detected in the proliferating region of the eye disc (H) and no transcripts are present in the postmitotic differentiating neurons posterior to morphogenetic furrow (asterisk in H). Note the reduction in DAxud1 levels in the region where the second mitotic wave occurs (arrowhead in I).

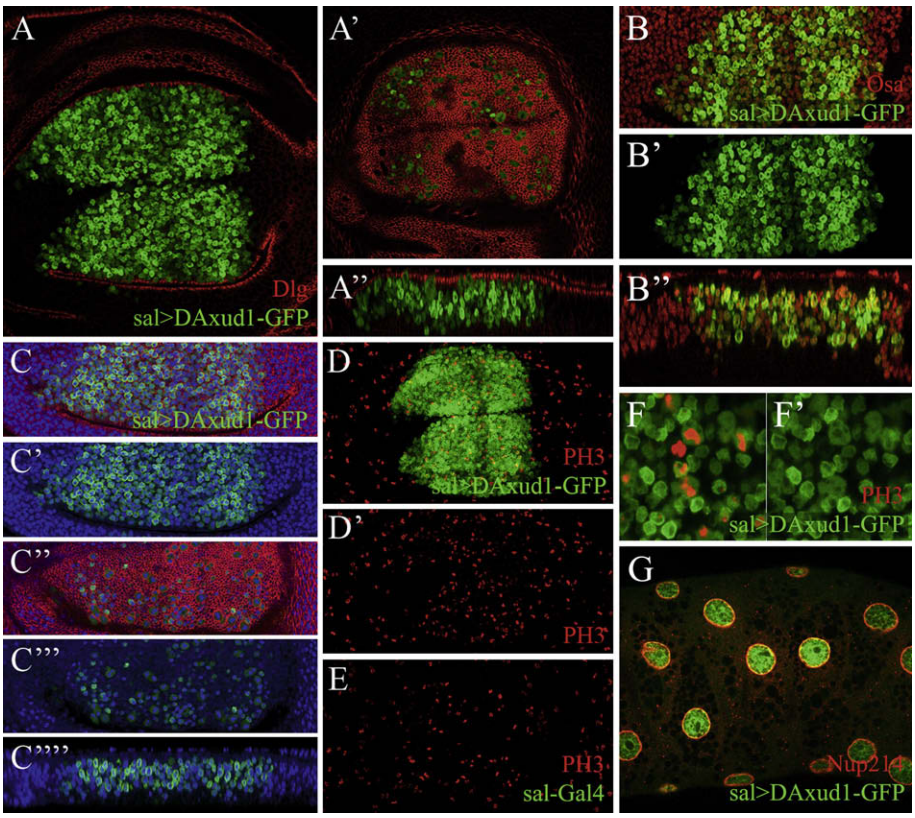

Fig. 2 – Sub-cellular localisation of DAxud1-GFP in the wing disc. (A-A") Expression of DAxud1-GFP (green) in *sal-Gal4/UAS-DAxud1-GFP* wing discs stained with the apical marker Disc large (red). The focal plane is medio-lateral in A and apical in A'. A" shown a Z-projection of the same disc. Cells in mitosis, localised in the apical side of the epithelium, show a diffuse appearance of DAxud1-GFP, whereas non-dividing cells have higher levels of DAxud1-GFP and preferential accumulation of the protein close to the nuclear envelope (see also H). (B-B") Expression of DAxud1-GFP (green) in *sal-Gal4/UAS-DAxud1-GFP* wing discs stained with an antibody against the nuclear protein Osa (red). B and B' show the dorsal compartment of the wing blade, and B' is the green channel. B" corresponds to Z-projection of the same disc. (C-C"") Expression of DAxud1-GFP (green) in *sal-Gal4/UAS-DAxud1-GFP* wing discs stained with the cell membrane marker FasIII (red) and the nuclear marker Topro (blue). C and C" are two different focal planes (C medio-lateral and C" apical) of the same disc and C"" is the corresponding Z-section showing only the blue (Topro) and green (DAxud1-GFP) channels. C' and C"' are the blue and green channels corresponding to C and C", respectively. (D, D') Expression of DAxud1-GFP (green) in *sal-Gal4/UAS-DAxud1-GFP* wing discs stained with the mitotic marker PH3 (red). (E) Expression of PH3 (red) in a *sal-Gal4* disc. Note the higher than normal accumulation of cells in mitosis in the domain of ectopic expression of DAxud1-GFP (compare the central region of D' and E). (F, F') Higher magnification (3x) of the dorsal side of a *sal-Gal4/UAS-DAxud1-GFP* wing disc stained with anti-PH3 (red). F' shown the green channel (DAxud1-GFP). (G) High magnification of a salivary gland of a *sal-Gal4/UAS-DAxud1-GFP* larva stained with anti-Nup214, a marker of the nuclear envelope. Note that the expression of Nup214 (red) envelops a ring of co-expression of Nup214 and DAxud1-GFP (yellow appearance).

co-localises in part with the nuclear envelope protein Nup214 (Fig. 2G).

To analyse the role of AXUD proteins during development and address its proposed function as tumour suppressor, we studied the consequences of reducing or increasing *DAxud1* expression in imaginal tissues combining the *UAS-DAxud1* and *UAS-iDAxud1* with different Gal4 lines. The specificity and capability of these constructs to increase *DAxud1* mRNA (*UAS-DAxud1*) and to evoke a RNA interference response, and thereby down regulate *DAxud1* function (*UAS-iDAxud1*), was confirmed by RT-PCR (Fig. 1C). Additionally, we confirmed the specificity of *iDAxud1* by its ability to revert the phenotype produced by *DAxud1* over-expression (see Fig. 5).

3.1. *DAxud1 modulates cell size and proliferation rate in Drosophila imaginal tissues*

Lowering *DAxud1* mRNA levels, by inducing the expression of *iDAxud1* in the posterior compartment of the wing disc (*hh-Gal4/UAS-iDAxud1*) generates flies with smaller than normal posterior compartments (Fig. 3B), without noticeable effects on wing patterning or cell differentiation. Region-specific size reductions can be elicited in combinations of *UAS-iDAxud1* with other Gal4 drivers, such as *ap-Gal4*, *sal-Gal4* or *ptc-Gal4*, in the corresponding domains of Gal4 expression (data not shown). To quantify the relative reduction in posterior compartment size and correct for individual variations in wing size, we determined the reduction in posterior compartment

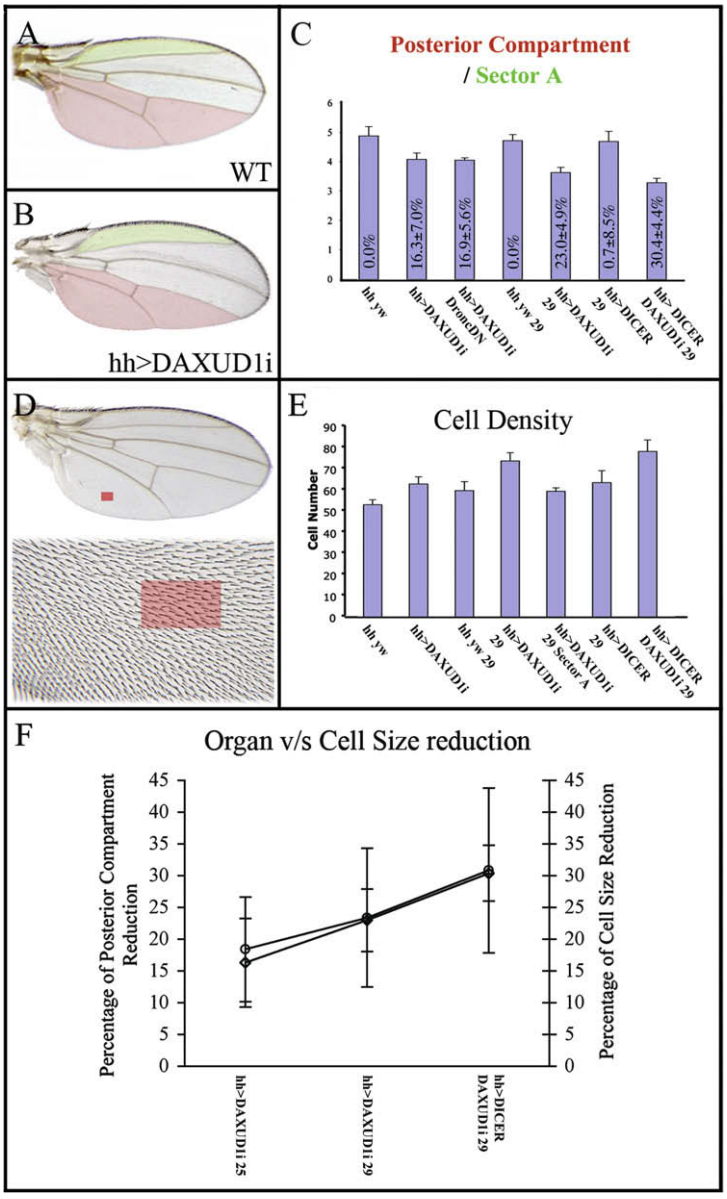

Fig. 3 – Organ and cell size adult phenotypes produced by decreasing *DAxud1* levels. (A) Control wing showing the regions used to quantify the effects of lowering *DAxud1* expression. The posterior compartment is shadowed in red and the L1-L2 intervein (sector A) is shadowed in green. (B) Wing phenotype generated by expression of *DAxud1* RNA interference in the posterior compartment (hh>DAXUD1i = *hh-Gal4/UAS-iDAxud1*). Note the reduction in the size of the posterior compartment. (C) Quantification of relative posterior compartment size reduction. Comparison of posterior compartment and sector A ratios of wild type and *hh-Gal4/UAS-DAxud1i* wings reveals a significant size reduction produced by diminishing *DAxud1* levels ($p<0.001$). This reduction is enhanced by co-expression with Dicer and is not affected by preventing apoptosis with a dominant negative form of Dronc ($Dronc^{DN}$, $p>0.1$). The number over each bar indicates the percentage of standardised posterior compartment reduction in experimental and control wings (*hh-Gal4/UAS-iDAxud1* relative posterior compartment size / WT at 25 °C or 29 °C relative posterior compartment size value). (D) Wild type wing (upper image) and an enlargement of sector E (lower image) showing the region (red square) from where wing hairs were counted. (E) Quantification of cell number in the area indicated as a red square in sector E (L5 to posterior wing margin). The number of cells, determined by counting single trichome produced by each cell, shows a substantial raise in cell number and therefore in cell density (at 25 °C *hh-Gal4/+* = 53 ± 2.37; *hh-Gal4/UAS-iDAxud1* = 62.76 ± 3.35; At 29 °C *hh-Gal4/+* = 59.63 ± 4.22; *hh-Gal4/UAS-iDAxud1* = 73.56 ± 3.90 in sector E and 59.33 ± 1.58 in sector A; *UAS-dicer/+; hh-Gal4/+* = 63.42 ± 5.55; *UAS-dicer; hh-Gal4/UAS-iDAxud1* = 78 ± 5.4). (F) Chart comparing the corresponding percentages of standardised reduction in standardised posterior compartment size and cell size. The reductions follow a linear relation matching each other in all analysed genotypes.

size as the ratio between the area of the posterior compartment (red area in Fig. 3A and B) and the area of sector A (green area in Fig. 3A and B). A significant reduction of relative posterior compartment area is observed in wings with lower levels of *DAxud1* ($p < 0.001$, Fig. 3C). The reduction in size is higher at 29 °C than 25 °C when comparing mutant (*hh-Gal4/UAS-iDAxud1*) and wild type posterior compartments, and this effect is stronger with the co-expression of the RNAse III Dicer ($p < 0.001$). In addition, no significant variation in the relative posterior compartment size reduction is detected when apoptosis is prevented in the posterior compartment by the co-expression of *iDAxud1* and a dominant negative form of the Caspase 9 Dronc (Igaki et al., 2002; Fig. 3C *p*-value>0.1 between *hh-Gal4/UAS-iDAxud1* and *hh-Gal4UAS-iDAxud1/UAS-Dronc^{DN}*); suggesting that the reduction of posterior compartment size is not produced by the apoptosis of cells expressing *iDAxud1*. We were unable to detect activated Caspase 3 or Acridine orange stain in *hh-Gal4/UAS-iDAxud1* wing discs and pupal wings (data not shown), confirming that cell death is not responsible for the reduction in size observed in the corresponding wings. The percentage of standardised reduction for posterior compartment sizes of *hh-Gal4/UAS-iDAxud1* and wild type wings (*hh-Gal4/UAS-iDAxud1* relative posterior compartment size/ WT relative posterior compartment size) are indicated in the chart (Fig. 3C).

Having excluded cell death, the reduction in wing size caused by lowering *DAxud1* levels could be generated by a combination of several mechanisms, including a decrease in cell size and/or cell proliferation. The analysis of cell numbers in adult wings was carried out by counting the hairs included in a particular wing region (red square in Fig. 3D), and shows a net increase in cell density in *hh-Gal4/UAS-iDAxud1* posterior compartments compared to wild type posterior compartments or to sector A of *hh-Gal4/UAS-iDAxud1* wings (Fig. 3E). The standardised cell density value in *hh-Gal4/UAS-iDAxud1* is 1.24 ± 0.11, which indicates that cells with decreased levels of DAxud1 are in average 24% smaller than wild type cells ($p < 0.0001$). This reduction increases to 31% in *UAS-dicer/+; hh-Gal4/UAS-iDAxud1* wings (hh > DICER + DAXUD1i = 1.31 ± 0.13). In this manner, the reduction in cell size accounts for the smaller posterior compartment size observed in *hh-Gal4/UAS-iDAxud1* wings, because the percentage of standardised reduction of posterior compartment sizes and percentages of standardised reduction in cell size match each other in all genotypes analysed (Fig. 3F).

To confirm that cell proliferation does not contribute to the phenotype of wings expressing *iDAxud1*, we monitored phospho-histone 3 (PH3) and the incorporation of BrdU in cells with reduced expression of DAxud1. Unexpectedly, the fraction of cells in the S phase of the cell cycle (BrdU positive) is higher than normal when DAxud1 levels are reduced (Fig. 4A, upper panel). Nevertheless, the amount of mitotic cells (PH3 positive) is not significantly modified in *iDAxud1* discs (Fig. 4A lower panel). Because the final number of cells is normal and cell death is not induced, it is likely that mutant cells spend more time than normal cells in phase S, in which case G1 and/or G2 should be shorter. Small effects on cell proliferation rhythms can be greatly amplified when cells of different genotypes are confronted in genetic mosaics (Morata and Ripoll, 1975; Moreno et al., 2002; Moreno and Basler, 2004). To compare the proliferation of cells with different DAxud1 levels in mosaics, we performed a MARCM clonal analysis (Lee and Luo, 1999). Wing discs of *y w hsFLP1.22/y w hsFLP1.22 TubGal4; UAS-GFP FRT42D/TubGal80 FRT42D; UAS-iDAxud1/+* genotype without heat sock treatment show generalised low levels of GFP expression, probably due to leaking in Gal80 repression (data not shown). This allows, after mitotic recombination, the visualisation of three cell populations: background cells (low GFP), homozygous *TubGal80 FRT42D* (twins, no expressing GFP) and homozygous *UAS-GFP FRT42D* cells expressing *UAS-iDAxud1* (clones, expressing higher levels of GFP). In the wild type situation, FLP-induced mitotic

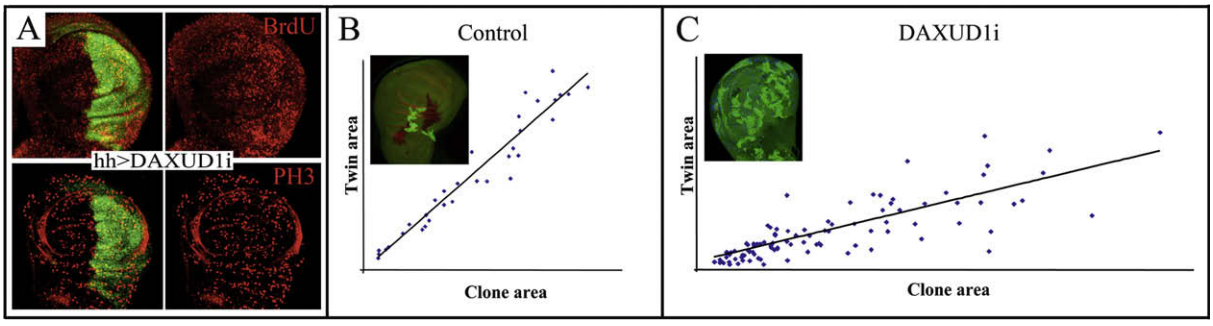

Fig. 4 – DAxud1 regulates the proliferation profile of imaginal cells. (A) Expression of BrdU (red, upper panels) and PH3 (red, lower panels) in *hh-Gal4 UAS-GFP / UAS-iDAxud1* (hh>DAXUD1i) wing discs. Note the increase in BrdU incorporation in the posterior compartment without changes in the number of PH3-expressing cells. Calculation of PH3 anterior/posterior compartment ratio within the wing pouch indicates that no significant variation occurs in the number of mitotic cell in *DAxud1* knockdown posterior compartments (control A/P ratio = 1.02 ± 0.10; experimental A/P ratio = 1.03 ± 0.07; p-value = 0.68). (B) Chart of control clone and twin areas of clones induced in *y w hsFLP1.22/ y w hsFLP1.22 TubGal4; UAS-GFP FRT42D/ TubGal80 FRT42D* wing discs at 48-72 h. AEL (Control). Note the nearly equal areas determined for each twin. (C) Chart of clone (lower DAxud1) and twin experimental areas induced in *y w hsFLP1.22/ y w hsFLP1.22 TubGal4; UAS-GFP FRT42D/ TubGal80 FRT42D; UAS-iDAxud1/+* (DAXUD1i). Clone area roughly doubles twin spot area at any clone size, showing the growth advantage acquired as a consequence of decreasing *DAxud1* function. Examples of control and experimental discs with clone-twin pairs are showed in the insets in B and C, respectively.

recombination induced in *y w hsFLP1.22/ y w hsFLP1.22 Tub-Gal4; UAS-GFP FRT42D/TubGal80 FRT42D* cells results in sister twin clones of similar size (Fig. 4B). In this manner, plotting the area occupied by sister twin clones generated at different developmental times fits a straight line ($r = 0.9999$) with a slope equal to 1 (Fig. 4B). In contrast, cells expressing *iDAxud1* generate clones larger than their respective twins. The clone-twin plot also generates a straight line ($r = 0.9999$), but clone area almost doubles twin area at each developmental time (Fig. 4C). These results indicate that cells with decreased levels of DAxud1 posses a proliferative advantage compared with surrounding cells expressing higher levels of DAxud1. This advantage is only revealed upon a confrontation of cells belonging to the same compartment and expressing different levels of DAxud1, and suggests a role of the protein to restrict cell proliferation in normal conditions.

3.2. *High levels of DAxud1 induce JNK-dependent apoptosis*

The human AXUD1 protein has been proposed to function as a tumour suppressor due to the reduction in its expression observed in cancers associated with mutations in the *AXIN* gene (Ishiguro et al., 2001). Common to tumour suppressors is their ability to restrict proliferation, and in several cases the increase in their activities lead to cell death. Our loss-of-function analysis has shown that DAxud1 is required to regulate proliferation rates and cell growth, thus defining final organ size. To further characterise DAxud1 activity we performed gain-of-function experiments. We used a P-GS insertion located 460 bp upstream of the *DAxud1* transcription start site (Fig. 1c-676). The *c-676* line is able to induce the expression of *DAxud1* when combined with wing and eye-specific Gal4 drivers (Fig. 5D and data not shown). Very similar phenotypes were obtained using the *c-676* line or a *UAS-DAxud1* construct in combination with a variety of Gal4 lines (data not shown). These phenotypes include a non-allometric reduction of wing size in *sal-Gal4/UAS-DAxud1* flies, which show a collapse of the L2/L3 intervein (Fig. 5B). Similarly, the eye is reduced in size in *ey-Gal4/UAS-DAxud1* individuals (Fig. 5C). These phenotypes were suppressed in combinations between the *c-676* line and the *UAS-iDAxud1* (Fig. 5J and data not shown). Considering our loss-of-function analysis and the proposed tumour suppressor activity of AXUD1, the tissue size reduction phenotypes could be the result of decreased cell proliferation and/or induction of cell death. Activated Caspase 3 and TUNEL staining show a robust apoptotic response in *DAxud1* over-expressing cells (Fig. 5E and F). The

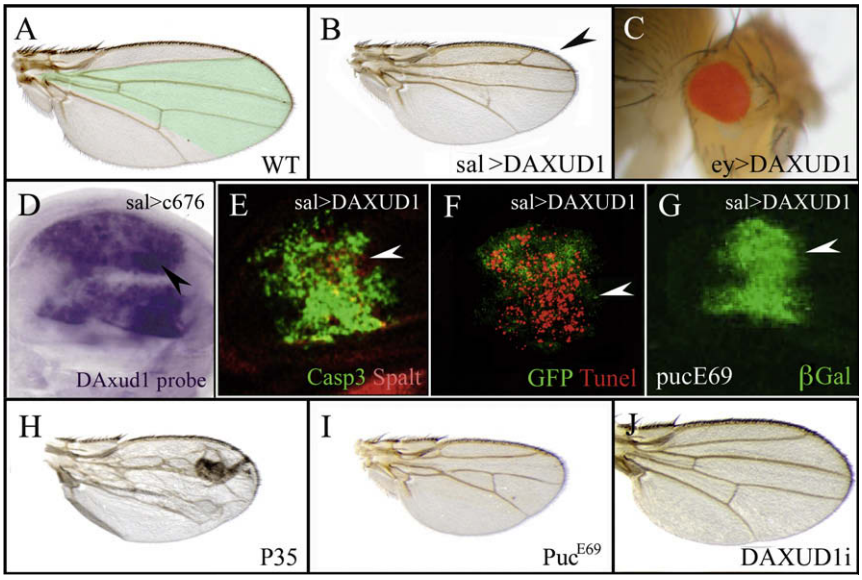

Fig. 5 – Over-expression of DAxud1 promotes apoptosis and activates the JNK pathway. (A) Wild type wing. (B) *sal-Gal4, UAS-DAxud1* (sal>DAXUD1) wing. Over-expression of *DAxud1* in the central region of the wing (L2 to L4, green domain in A) produces a non-allometric reduction in size and the collapse of the L2-L3 intervein (arrowhead). (C) *ey-Gal4/UAS-DAxud1* (ey>DAXUD1) eye showing a reduction in organ size. (D) In situ hybridization of *DAxud1* in a wing disc of *sal-Gal4/c-676* genotype, showing the strong expression of *DAxud1* induced in the Gal4 expressing cells. (E) Expression of DAxud1 in the *sal-Gal4* domain (*sal-Gal4, UAS-DAxud1*) leads to a robust activation of Caspase3 (green) in third instar wing discs (arrowhead). The expression of *Spalt* is shown in red. (F) Cells positive for TUNEL staining (red) are detected in *sal-Gal4/UAS-DAxud1; UAS-GFP/+* wing discs (arrowhead). The expression of GFP is in green. (G) Puckered expression (green) is induced in the central region of *sal-Gal4/UAS-DAxud1; puc-lacZ^{E69}/+* wing discs by *DAxud1* over-expression (arrowhead). (H) Adult wing of *sal-Gal4/UAS-DAxud1; UAS-p35/+* genotype. Co-expression of *DAxud1* and *p35* partially reverts *DAxud1* phenotype and produces epithelial extrusion in the adult wing. (I) Adult wing of *sal-Gal4/UAS-DAxud1; puc-lacZ^{E69}/+* genotype. The expression of *DAxud1* in a heterozigous *puckered* (puc^{E69}) background significantly enhances the wing phenotype (compare to B). (J) Adult wing of *sal-Gal4/c-676; UAS-iDAxud1/+* genotype. The co-expression of *DAxud1* (*c-676*) and *DAxud1* RNA interference construct (DAXUD1i= *iDAxud1*) suppresses the observed phenotype. Larvae were grown at 29 °C with the exception of those of D, which were incubated at 25 °C.

JNK pathway has been implicated in apoptotic responses in cell competition assays and during normal morphogenetic processes in *Drosophila* (Moreno et al., 2002; Lee et al, 2005; Balakireva et al., 2006; Manjon et al., 2007). Using the puc^{E69} enhancer trap line (Martin-Blanco et al., 1998) we were able to detect *puc* induction in cells expressing high levels of *DAxud1* (Fig. 5G). To get insight about the contribution of cell death to the adult phenotype produced by *DAxud1* over-expression we blocked apoptosis co-expressing DAxud1 with the anti-apoptotic protein p35, which blocks Caspase 3 activation (Fig. 5H). The adult wing phenotype produced by DAxud1 over-expression was only partially corrected in this genetic combination, suggesting that additional processes, perhaps proliferation rates, are compromised under these circumstances. To confirm whether cell death is the result of JNK pathway activation we performed genetic interactions with mutations in genes belonging to the JNK pathway. Partial reversion of the wing phenotype generated by ectopic *DAxud1* was detected in genetic combinations of with a null *Hemipterous* allele in heterozygosity (Hep^{r75}; JNK-Kinase, JNKK) and with a *Basket* hypomorph allele (Bsk^{J27}; Jun NH_2-terminal Kinase, JNK) (data not shown). Conversely, decreasing the levels of *puc* (puc^{E69}/+), the phosphatase that negatively regulates Bsk activity, causes a reduction in wing size stronger than only increasing DAxud1 (Fig. 5I). The JNK pathway and apoptosis are also activated in cells with reduced Decapentaplegic (Dpp) or Wingless (Wg) signalling, which are thereby eliminated from the wing epithelium (Adachi-Yamada et al., 1999; Moreno et al., 2002; Gibson and Perrimon, 2005). Analysis of the expression of downstream targets of Dpp and Wg, like phospho-Mad, Spalt or Distalless, shows that the apoptosis evoked by DAxud1 is not due to impairing *dpp* or *wg* signalling (Suppl. Fig. 1).

3.3. *DAxud1 regulates apoptosis versus cell cycle progression in a Cdk1-dependent process*

Several tumour suppressors regulate proliferation by modulating the activity of essential cell cycle elements such as the Cyclin E/Cdk2 complex, the E2F1 transcription factor and the Cdc25/*String* phosphatase. Blockage of cell cycle can promote apoptosis in a cell autonomous fashion or alternatively, as a result of cell competition by the surrounding cells (Basu et al., 1999; Prober and Edgar, 2000; Migeon et al., 1999; Pellock et al., 2007). To define whether the adult phenotype and apoptosis induced by DAxud1 over-expression during larval stages is the consequence of alterations in cell cycle control, we monitored the expression of markers specific of different phases of the cell cycle. Analysis of BrdU incorporation in wing discs expressing high levels of *DAxud1* shows that the number of cells is S phase is severely reduced (Fig. 6C, C'). In contrast, the number of cells positive for the mitotic marker PH3 is increased (93.13 ± 14.7 $n = 16$ Fig. 6E, E' and F) compared with wild type third instar larval wing discs (Fig. 6D and D' 48 ± 6.75 $n = 10$). The increase in mitotic cell numbers and the BrdU incorporation blockage is not modified by the expression of the anti-apoptotic protein p35 (82.34 ± 12.64 $n = 12$; Fig. 6I and H). Thus, the abnormally high number of PH3-expressing cells seems to correspond to cells accumulating in mitosis, and not a consequence of compensatory proliferation triggered by apoptosis. A fraction of cells stained for PH3 is also positive for TUNEL (Fig. 6G), suggesting that apoptosis is initiated in cells stopped in mitosis by high levels of DAxud1. Ectopic expression of the DAxud1-GFP fusion protein also increases the number of cells in mitosis expressing PH3 in *sal-Gal4/UAS-DAxud1-GFR* discs (Fig. 2D and E). Interestingly, the accumulation of DAxud1-GFP is reduced in mitotic cells expressing PH3 (Fig. 2F).

Eye development offers a system where cells enter the cell cycle co-ordinately during the second mitotic wave, whereas cells posterior to this mitotic domain are post mitotic. The ectopic expression of DAxud1 in cells posterior to the morphogenetic furrow in the eye disc (*GMR-Gal4/c-676*) produces a strong increase in PH3-expressing cells (Fig. 6K) compared with wild type eye discs (Fig. 6J) without affecting BrdU incorporation (Fig. 6L). In addition, the accumulation of PH3 positive cells is associated with a robust induction of apoptosis in these cells (Fig. 6M). Thus, it seems that cells expressing higher than normal levels of *DAxud1* enter apoptosis as a result of a mitotic blockage of the second mitotic division. The differentiation of photoreceptors in *GMR-Gal4/c-676* eye discs is normal as monitored by the expression of Elav (Fig. 6K and M).

To further define the effects on apoptosis and cell cycle progression caused by higher than normal levels of DAxud1, we performed a gain-of-function clonal analysis. DAxud1 over-expressing clones, induced at 36 ± 12, 60 ± 12 or 84 ± 12 AEL, were not found in third instar larva wing imaginal discs (data not shown), suggesting that DAxud1 over-expression imposes a proliferation disadvantage, possibly due to apoptosis induction, that eliminates these cells from proliferating tissues.

To identify candidate targets of DAxud1 mediating its effects in cell cycle progression, we analysed the adult phenotype, and the number of mitotic cells and apoptosis in the corresponding imaginal disc, of combinations between DAxud1 and Cdk1 or String/Cdc25. Cdk1 is important for the G2/M transition and functions as the catalytic subunit of the Cdk1/CycB complex. Interestingly, the co-expression of DAxud1 with Cdk1 almost completely reverts the adult phenotype produced by ubiquitous expression of DAxud1 in the wing (Fig. 7B compare with Fig. 7A). As expected from this suppression, apoptosis and accumulation of PH3 positive cells is nearly normal in wing discs co-expressing DAxud1 and Cdk1 (59 ± 7.99 $n = 12$ Fig. 7C, C'; E, E' and G, G'). Co-expression of DAxud1 with String (Fig. 7D, D'; F, F' and H, H') or Cyclin B (data not shown) does not prevent PH3 accumulation (Stg: 98 ± 7.07 $n = 14$, CycB: 83 ± 9.34 $n = 12$) and apoptosis. Furthermore, the heterozygosity of *String* (Stg^4/+) or *Cyclin B1* ($CycB^2$/+) does not modify the adult phenotype or the induction of apoptosis caused by DAxud1 (not shown). In addition, changes in the activity of the Cdk1/CycB regulators Wee1 or Myt1 do not modify the DAxud1 over-expression phenotype (data not shown). Therefore the effect of Cdk1 levels on DAxud1 is not reproduced by String/Cdc25-mediated activation of the Cdk1/CycB complex or through the modification of Cyclin B levels. Finally, the over-expression of G1/S promoting factors such as E2F/Dp complex or Cdk2 slightly enhance the effects of DAxud1 over-expression (data not shown). These later results suggest that DAxud1 specifically reduces

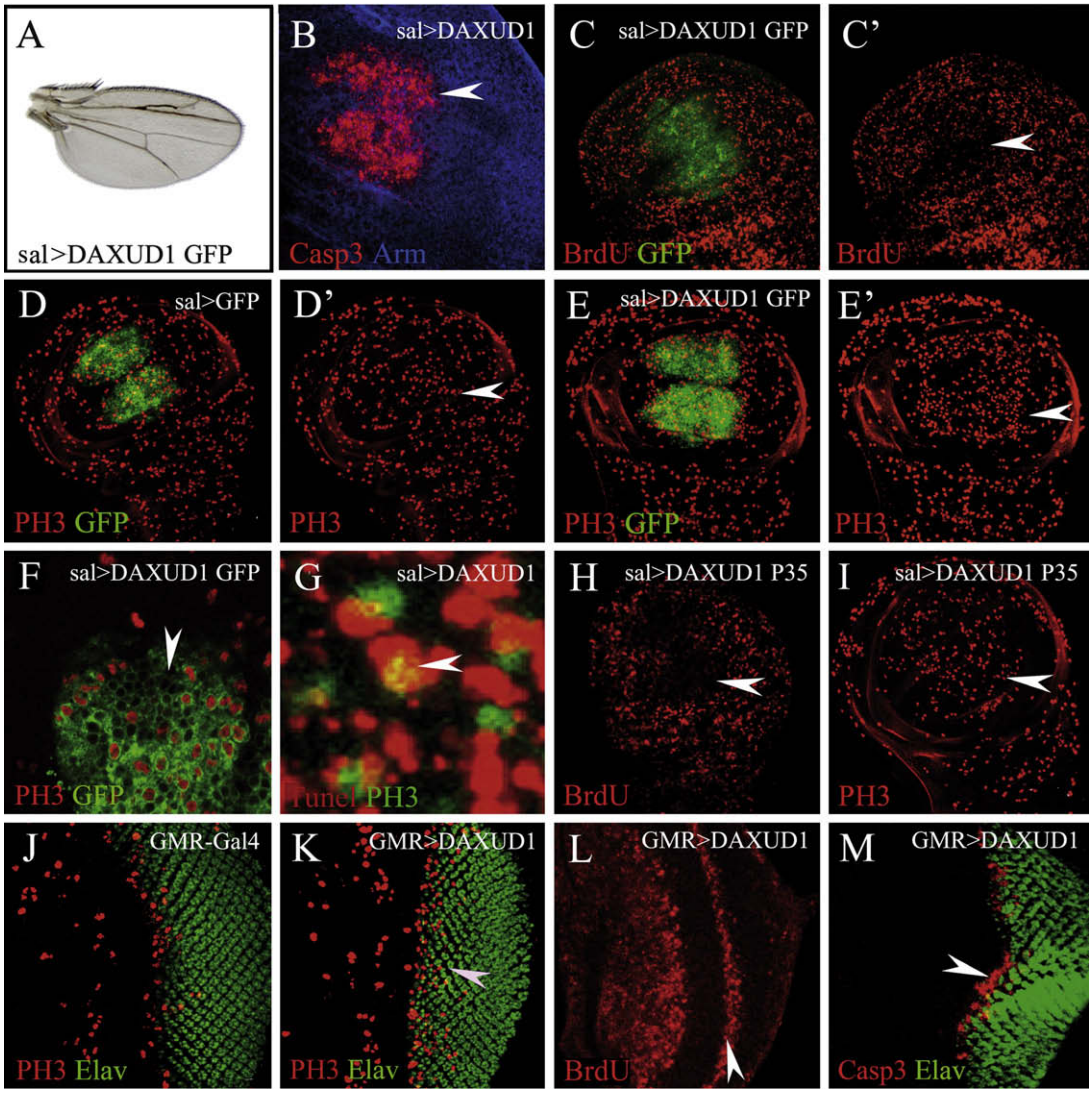

Fig. 6 – Increased expression of DAxud1 blocks the cell cycle during mitosis. (A) Wing phenotype produced by *sal-Gal4* directed co-expression of DAxud1 and CD8-GFP. (B) Caspase 3 (red) is activated in the corresponding wing discs. Armadillo expression is shown in blue. (C, C') BrdU incorporation (red) is impaired (arrowhead in C') in DAxud1-expressing cells (green). (D, D') Control wing disc (*sal-Gal4/UAS-CD8::GFP*) stained for phospho-histone 3 (PH3 in red). (E, E') Augmented number of PH3 positive cells (red) in the *sal* expressing domain (green) in *sal-Gal4 UAS-DAxud1/UAS-CD8::GFP* wing discs. (F) Higher magnification showing the increase in mitotic cells within the *DAxud1* over-expression territory (arrowhead) in *sal-Gal4 UAS-DAxud1/UAS-CD8::GFP* discs. (G) TUNEL staining (red) and PH3 (green) co-localise in a fraction of DAxud1-expressing cells (arrowhead). (H, I) BrdU incorporation (H) and PH3 accumulation (I) are still affected in the DAxud1-expressing domain (arrowhead) of *sal-Gal4 UAS-DAxud1/UAS-p35* discs, even though cell death is prevented through p35 expression. (J) Control eye disc stained for Elav (green) and PH3 (red). (K, L) Expression of *DAxud1* posterior to morphogenetic furrow (*GMR-Gal4/c-676*, arrowhead) influences PH3 staining at the second mitotic wave without affecting BrdU incorporation or differentiation profiles in this territory. (M) Robust Caspase 3 activation is detected posterior to morphogenetic furrow (arrowhead), exclusively where the second mitotic division takes place (arrowhead). Scale bar (A) = 700 μm; (B, J, K, L, M) = 50 μm; (C, C', D, D', E, E', H, I) = 100 μm; (F) = 10 μm; (G) 1,5 μm.

Cdk1-mediated activity during mitosis. The fact that Cdk1 hypomorphic alleles prevent mitosis completion without affecting DNA replication (Weigmann et al., 1997), together with the observation that co-expression of DAxud1 and Cdk1 completely reverts DAxud1-over-expression outcomes suggests that DAxud1 might repress *cdc2* expression or reduce Cdk1 activity. We were not able to detect changes in *cdc2* RNA expression levels using a RT-PCR approach in wing discs with augmented expression of DAxud1 (data not shown), suggesting that DAxud1 antagonises Cdk1 activity.

4. Discussion

Organ size depends on rates of cell proliferation, cell growth and cell death. Unbalance of these processes could lead to massive cell death or to hyperplasic growth, which un-

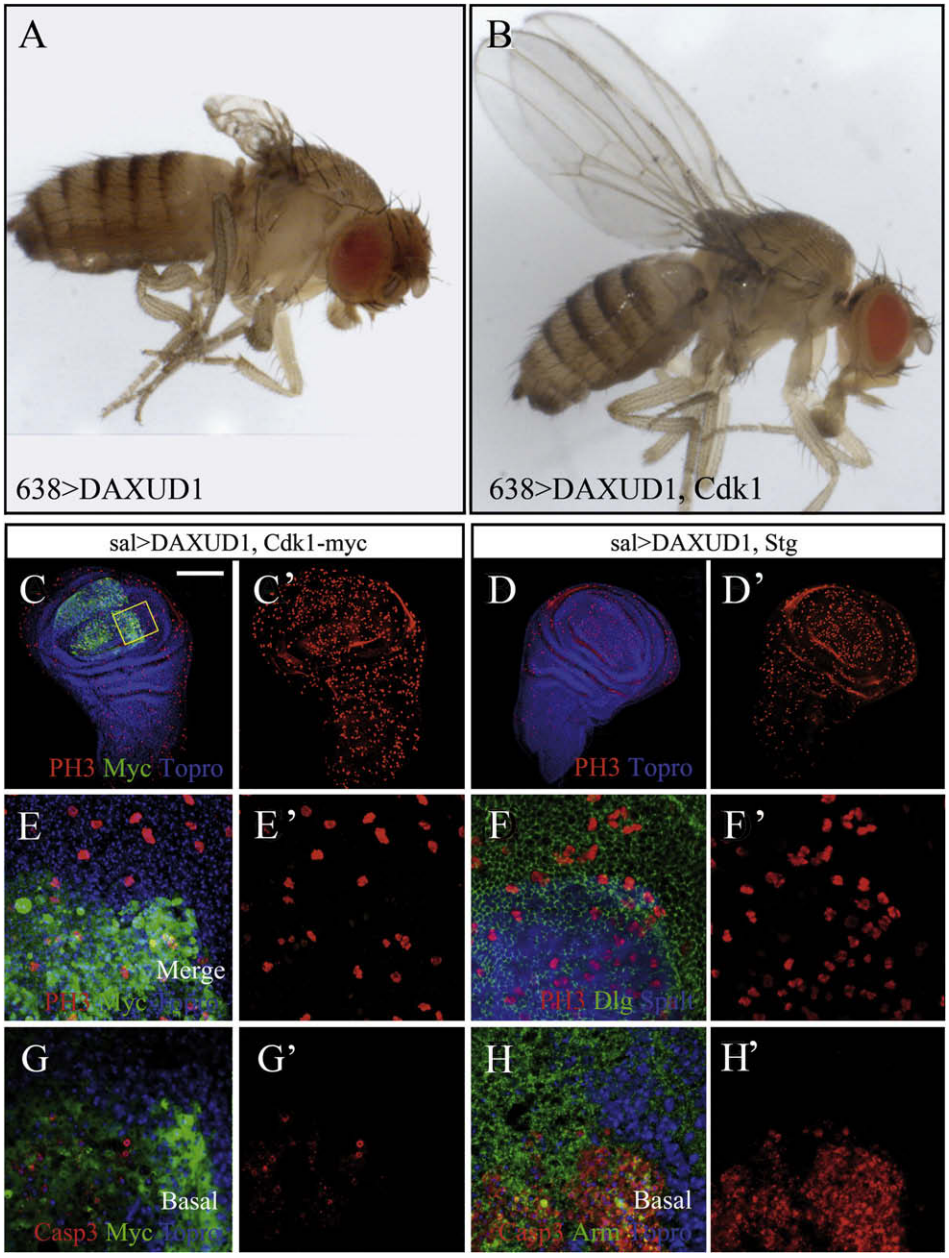

Fig. 7 – Effects of Cdk1 and String on the induction of apoptosis and cell cycle effects by *DAxud1*. (A, B) Abolition of DAxud1 ectopic expression phenotype by Cdk1 co-expression. Generalised over-expression of DAxud1 in the wing strongly impairs wing development (A). Note the cancellation of DAxud1 phenotype when Cdk1 is co-expressed (B). (C, C', E, E' and G, G'). Wing discs of the *sal-Gal4 UAS-DAxud1/UAS-Cdk1-myc* genotype. (C, C', E, E') The accumulation of PH3 and apoptosis (E, E' and G, G') are cancelled by co-expression of DAxud1 and Cdk1 in *sal-Gal4 UAS-DAxud1/UAS-Cdk1-myc* discs compared to DAxud1 over-expression in *sal-Gal4 UAS-DAxud1* discs (compare with Fig. 6E and F). (D, D', F, F' and H, H') Wing discs of the *sal-Gal4 UAS-DAxud1/UAS-Stg* genotype. String co-expression does not modify the outcomes produced by *DAxud1* over-expression in *sal-Gal4 UAS-DAxud1/UAS-Stg* discs. Note the reduction in Caspase 3 stain in G' compared with H'. (E-H') Correspond to magnifications of the wing pouch area indicated in yellow in panel C; the images have been rotated so that the side pointing towards the centre of the disc (the *sal-Gal4* expressing domain) is to the bottom of each panel. Co-expression of DAxud1 with Cdk1 or String was performed at 29 °C to obtain the strongest DAxud1 responses. Scale bar (A, B) = 350 μm; (C, C', D, D') = 100 μm; (E, E', F, F', G, G', H, H') = 15 μm.

der certain conditions develops as tumours. A key aspect of growth control is the regulation of cell cycle progression, as modifications in cell cycle regulators have been demonstrated to cause unrestricted growth and metastasic behaviour in *Drosophila* imaginal cells (Huang et al., 2005, reviewed by Pan, 2007 and references therein). We have investigated the function of *Drosophila Axud1* during development, focusing on its effects on cell division and apoptosis in imaginal discs. Our phylogenetic analysis, together with the conserved protein features described by Gingras et al. demonstrate that

AXUD proteins (CSRNP in mice) have been conserved through evolution. Protein sequence comparison shows that these nuclear proteins posses a stretch of Cysteine residues of variable length common to all species analysed. Although a functional analysis of this domain is still missing, the structural hallmarks of AXUD proteins suggest they constitute a novel conserved family of transcription factors.

4.1. *DAxud1 behaves as a JNK-dependent pro-apoptotic factor*

To address the function of *DAxud1* we opted for an in vivo approach using both loss- and gain-of-function experiments. Over-expression analysis in imaginal discs revealed that excess of *DAxud1* impairs organ development, causing a reduction in organ size. Cell death analysis in these tissues indicates that DAxud1 over-expression consistently activates apoptosis, indicating that size reduction can be attributed in part to a diminution in cell number. Several experimental situations that lead to apoptosis in imaginal discs, including morphogenetic apoptosis, implicate the inappropriate activation of the JNK pathway (Adachi-Yamada et al., 1999; Moreno et al., 2002; Ryoo et al., 2004; Lee et al., 2005). We found that the adult wing phenotype caused by *DAxud1* over-expression is accompanied with the activation of the JNK pathway in the wing disc. Accordingly, this phenotype is partially reverted in heteroallelic combinations with several components of the JNK pathway or by expressing its negative regulator. Taken together, these results suggest that DAxud1 pro-apoptotic effect is caused by the activation of the JNK pathway in imaginal cells.

4.2. *Apoptosis is induced by a blockage in Mitosis in a Cdk1-dependent process*

Since activation of the Dpp and Wg pathways are necessary for normal wing disc development, the cell death elicited by DAxud1 could be a consequence of an inhibitory effect on these pathways (Gibson and Perrimon, 2005; Adachi-Yamada and O'Connor, 2002). However, no effects were detected in the expression of Dpp and Wg target genes, indicating that DAxud1 functions independently of Dpp and Wg activity. Due to the proposed role as a tumour suppressor for AXUD1, we studied the function of *DAxud1* in cell cycle progression, observing a blockage in proliferation accompanied by the accumulation of cells in mitosis. The reduced levels of BrdU incorporation and the concomitant increase in the number of PH3 positive cells could arise from an extremely fast progression through the cell cycle. Because we performed a relatively short BrdU pulse (30 min) and the tissue was immediately fixed afterwards, it is very unlikely that mitotic dilution of BrdU explains our observation. Since DAxud1 also promotes apoptosis, compensatory proliferation (Ryoo et al., 2004) and cell competition (Morata and Ripoll, 1975) could account for the higher amount of PH3 positive cells within DAxud1-expressing domain. However, reduced BrdU incorporation and high number of PH3 positive cells are observed in wing discs co-expressing DAxud1 and the apoptotic inhibitor p35, strongly arguing against both alternatives. We suggest that increasing DAxud1 retards or blocks some stage during mitosis and consequently reduces proliferation. This blockage leads to a JNK-dependent apoptosis, a possibility supported by the following observations: decreasing JNK activity in heteroallelic combinations reduces the DAxud1 over-expression phenotype, a fraction of TUNEL positive cells express PH3 and the pro-apoptotic effects of DAxud1 are suppressed by Cdk1 expression. In addition, the expression of E2F/Dp or Cdk2, which accelerate the G1/S transition, cause stronger cell death and higher accumulation of PH3 positive cells (not shown). This is likely a consequence of more cells reaching mitosis, and them becoming affected by the blocking activity of DAxud1. In our rescue experiments, expression of Cdk1 is unlike to cause changes in Cyclin B or Cdc25/String phosphatase, suggesting that a CycB/Cdk1-independent process is the target of DAxud1 activity. Analysis of Cdk1 function in *Drosophila* imaginal cells, using the hypomorph temperature-sensitive allele $Cdc2^{E1\text{-}24}$ has shown that reduction in its activity leads to mitotic blockage (Weigmann et al., 1997). However $cdc2^{E1\text{-}24}$ cells progress to DNA replication, endoreplicating their DNA and acquiring higher cell size (Weigmann et al., 1997). In our results, DAxud1 over-expression likewise impairs mitotic progression but no endoreplication is detected. A possible explanation is that DAxud1 over-expression represses very effectively Cdk1 activity, reducing Cdk1 function below the levels reached by the $Cdc2^{E1\text{-}24}$ allele. In this manner, these cells became blocked in mitosis without progressing to endoreplicative cycles. This reasoning also explains the inability of CycB to rescue DAxud1 over-expression and the exclusive role of Cdk1 to revert the DAxud1 over-expression phenotype. Finally, the effects of DAxud1 over-expression are restricted to mitotically active tissues, as no significant apoptosis or differentiation defects are detected when DAxud1 is expressed, for example, in cells posterior to the second mitotic wave domain in the eye disc.

The observed restriction imposed by DAxud1 upon mitosis progression implies that cells where the activity of this gene is decreased should exhibit a proliferative advantage. This is indeed what we observed in cells after knocking down *DAxud1*, which increases proliferation as detected by BrdU incorporation. These mutant cells also display a reduction in cell size, which finally result in a smaller wing posterior compartment size. The reduction in cell size could be a consequence of reduced length of G1 and/or G2, or, alternatively, it might imply a function of the protein in the signalling pathways that regulate cell size. We have not addressed the mechanisms by which *DAxud1* influences cell size.

It is remarkable that the reduction of *DAxud1* expression confers cells a proliferation advantage, as observed in twin analysis. Thereby, cells with decreased levels of *DAxud1* behave as cells with increased mitogenic potential. This behaviour, together with the consequences of increasing DAxud1 levels, lead to the hypothesis that DAxud1 might antagonize the effect of pro-proliferative signals in proliferating cells. In this manner, DAxud1 might act as a sensor of pro-proliferative inputs within the cell that imposes a restriction of progression through mitosis. When over-expression of DAxud1 breaks this balance cells triggers JNK-dependent apoptosis. Recently, Gingras et al. described the transcriptional activator ability and individual knockouts for the orthologues of DAxud1 in mice (CSRNP-1, -2 and –3) (Gingras et al., 2007). They

did not detect any obvious effects on mouse development, hematopoiesis or T cell functions. Interestingly, CSRNP-1 was cloned from IL-2 treated T-cells, a general pro-mitogenic signal for these cells. The apparent discrepancy between the lack of phenotypes in knockout mice and the requirement of *Drosophila* DAxud1 might rely on redundancy among proliferation control mechanisms in mice. We did not detect tumoural behaviour in cells with lower *DAxud1* levels, as might be expected from the proposed function of human AXUD as a tumour suppressor (Ishiguro et al., 2001). The proliferation advantage of cells with lower levels of DAxud1 in genetic mosaics is compatible with a facilitating role in tumour progression, although to generate hyperplasic proliferation other priming pro-tumourigenic events must occur in the cell. The effects of DAxud1 in cell viability; cell competition and cell cycle progression identified in imaginal cells should open new avenues to understand the function of this family of related proteins during development and cancer progression.

Acknowledgments

We would like to thank Dr. Campbell for providing the *UAS-Wee* and *UAS-Myt* fly stocks, Miguel Allende, Antonio Baonza and Francisco Martín for critical reading and insights during the preparation of this manuscript, and Christos Samakovlis, the Bloomington stock center and the Hybridoma bank for fly stocks and reagents. The help of Marcos Mendez with the phylogenetic analysis and the technical assistance of Patricio Olguín is also acknowledged. We are especially grateful to Beatriz Pérez and Antonio Baonza for the gift of the image shown in Fig. 6K. This work was funded by FONDECYT (3050042) and ICM P06-039 grants to A.G. and by a BFU2006-06501 grant of the M.E.C. to J.F.dC.

Appendix A. Supplementary data

Supplementary data associated with this article can be found, in the online version, at doi:10.1016/j.mod.2008.11.005.

REFERENCES

Adachi-Yamada, T., Fujimura-Kamada, K., Nishida, Y., Matsumoto, K., 1999. Distortion of proximodistal information causes JNK-dependent apoptosis in *Drosophila* wing. Nature 400, 166–169.

Adachi-Yamada, T., O'Connor, M.B., 2002. Morphogenetic apoptosis: a mechanism for correcting discontinuities in morphogen gradients. Dev. Biol. 251 (1), 74–90.

Ae, K., Kobayashi, N., Sakuma, R., Ogata, T., Kuroda, H., Kawaguchi, N., Shinomiya, K., Kitamura, Y., 2002. Chromatin remodeling factor encoded by ini1 induces G1 arrest and apoptosis in ini1-deficient cells. Oncogene 21 (20), 3112–3120.

Balakireva, M., Rosse, C., Langevin, J., Chien, Y.C., Gho, M., Gonzy-Treboul, G., Voegeling-Lemaire, S., Aresta, S., Lepesant, J.A., Bellaiche, Y., White, M., Camonis, J., 2006. The Ral/exocyst effector complex counters c-Jun N-terminal kinase-dependent apoptosis in *Drosophila melanogaster*. Mol. Cell. Biol. 26 (23), 8953–8963.

Barrio, R., de Celis, J.F., Bolshakov, S., Kafatos, F.C., 1999. Identification of regulatory regions driving the expression of the *Drosophila* spalt complex at different developmental stages. Dev. Biol. 215 (1), 33–47.

Basu, J., Bousbaa, H., Logarinho, E., Li, Z., Williams, B.C., Lopes, C., Sunkel, C.E., Goldberg, M.L., 1999. Mutations in the essential spindle checkpoint gene bub1 cause chromosome missegregation and fail to block apoptosis in *Drosophila*. J. Cell. Biol. 146 (1), 13–28.

Bhat, K.M., Apsel, N., 2004. Upregulation of Mitimere and Nubbin acts through cyclin E to confer self-renewing asymmetric division potential to neural precursor cells. Development 131 (5), 1123–1134.

Blom, N., Gammeltoft, S., Brunak, S., 1999. Sequence- and structure-based prediction of eukaryotic protein phosphorylation sites. J. Mol. Biol. 294 (5), 1351–1362.

Buffin, E., Emre, D., Karess, R.E., 2007. Flies without a spindle checkpoint. Nat. Cell Biol. 9 (5), 565–572.

de Celis, J.F., 1997. Expression and function of decapentaplegic and thick veins during the differentiation of the veins in the *Drosophila* wing. Development 124 (5), 1007–1018.

Duronio, R.J., Bonnette, P.C., O'Farrell, P.H., 1998. Mutations of the *Drosophila* dDP, dE2F, and cyclin E genes reveal distinct roles for the E2F-DP transcription factor and cyclin E during the G1-S transition. Mol. Cell. Biol. 18 (1), 141–151.

Gelbart, W.M., Crosby, M., Matthews, B., Rindone, W.P., Chillemi, J., Russo Twombly, S., Emmert, D., Ashburner, M., Drysdale, R.A., Whitfield, E., Millburn, G.H., de Grey, A., Kaufman, T., Matthews, K., Gilbert, D., Strelets, V., Tolstoshev, C., 1997. FlyBase: a *Drosophila database*. The FlyBase consortium. Nucleic Acids Res. 25 (1), 63–66.

Gibson, M.C., Perrimon, N., 2005. Extrusion and death of DPP/BMP-compromised epithelial cells in the developing *Drosophila* wing. Science 307, 1785–1789.

Gingras, S., Pelletier, S., Boyd, K., Ihle, J.N., 2007. Characterization of a Family of Novel Cysteine- Serine-Rich Nuclear Proteins (CSRNP). PLoS ONE 2 (8), e808.

Hamaratoglu, F., Willecke, M., Kango-Singh, M., Nolo, R., Hyun, E., Tao, C., Jafar-Nejad, H., Halder, G., 2006. The tumour-suppressor genes NF2/Merlin and Expanded act through Hippo signalling to regulate cell proliferation and apoptosis. Nat. Cell Biol. 8 (1), 27–36.

Huang, H., Potter, C.J., Tao, W., Li, D.M., Brogiolo, W., Hafen, E., Sun, H., Xu, T., 1999. PTEN affects cell size, cell proliferation and apoptosis during *Drosophila* eye development. Development 126 (23), 5365–5372.

Huang, J., Raff, J.W., 1999. The disappearance of cyclin B at the end of mitosis is regulated spatially in *Drosophila* cells. EMBO J. 18 (8), 2184–2195.

Huang, J., Wu, S., Barrera, J., Matthews, K., Pan, D., 2005. The Hippo signaling pathway coordinately regulates cell proliferation and apoptosis by inactivating Yorkie, the *Drosophila* Homolog of YAP. Cell 122 (3), 421–434.

Huang, H., He, X., 2008. Wnt/beta-catenin signaling: new (and old) players and new insights. Curr. Opin. Cell Biol. 20 (2), 119–125.

Igaki, T., Kanda, H., Yamamoto-Goto, Y., Kanuka, H., Kuranaga, E., Aigaki, T., Miura, M., 2002. Eiger, a TNF superfamily ligand that triggers the *Drosophila* JNK pathway. EMBO J. 21 (12), 3009–3018.

Ishiguro, H., Tsunoda, T., Tanaka, T., Fujii, Y., Nakamura, Y., Furukawa, Y., 2001. Identification of AXUD1, a novel human gene induced by AXIN1 and its reduced expression in human carcinomas of the lung, liver, colon and kidney. Oncogene 20 (36), 5062–5066.

Knoblich, J.A., Sauer, K., Jones, L., Richardson, H., Saint, R., Lehner, C.F., 1994. Cyclin E controls S phase progression and its down-regulation during *Drosophila* embryogenesis is required for the arrest of cell proliferation. Cell 77 (1), 107–120.

Lee, L.A., Orr-Weaver, T.L., 2003. Regulation of cell cycles in *Drosophila* development: intrinsic and extrinsic cues. Annu. Rev. Genet. 37, 545–578.

Lee, S.B., Park, J., Jung, J.U., Chung, J., 2005. Nef induces apoptosis by activating JNK signaling pathway and inhibits NF-kappaB-dependent immune responses in *Drosophila*. J. Cell Sci. 118, 1851–1859.

Lee, T., Luo, L., 1999. Mosaic analysis with a repressible cell marker for studies of gene function in neuronal morphogenesis. Neuron 22 (3), 451–461.

Leevers, S.J., McNeill, H., 2005. Controlling the size of organs and organisms. Curr. Opin. Cell Biol. 17 (6), 604–609.

Leismann, O., Lehner, C.F., 2003. *Drosophila* securin destruction involves a D-box and a KEN-box and promotes anaphase in parallel with Cyclin A degradation. J. Cell Sci. 116, 2453–2460.

Manjon, C., Sanchez-Herrero, E., Suzanne, M., 2007. Sharp boundaries of Dpp signalling trigger local cell death required for *Drosophila* leg morphogenesis. Nat. Cell Biol. 9 (1), 57–63.

Margottin-Goguet, F., Hsu, J.Y., Loktev, A., Hsieh, H.M., Reimann, J.D., Jackson, P.K., 2003. Prophase destruction of Emi1 by the SCF(betaTrCP/Slimb) ubiquitin ligase activates the anaphase promoting complex to allow progression beyond prometaphase. Dev. Cell 4 (6), 813–826.

Martin-Blanco, E., Gampel, A., Ring, J., Virdee, K., Kirov, N., Tolkovsky, A.M., Martinez-Arias, A., 1998. Puckered encodes a phosphatase that mediates a feedback loop regulating JNK activity during dorsal closure in *Drosophila*. Genes Dev. 12 (4), 557–570.

Mata, J., Curado, S., Ephrussi, A., Rørth, P., 2000. Tribbles coordinates mitosis and morphogenesis in *Drosophila* by regulating string/CDC25 proteolysis. Cell 101 (5), 511–522.

Migeon, J.C., Garfinkel, M.S., Edgar, B.A., 1999. Cloning and characterization of peter pan, a novel *Drosophila* gene required for larval growth. Mol. Biol. Cell 10 (6), 1733–1744 (Mol. Cell. Biol. 26(23):8953–8963).

Molnar, C., Lopez-Varea, A., Hernandez, R., de Celis, J.F., 2006. A gain-of-function screen identifying genes required for vein formation in the *Drosophila melanogaster* wing. Genetics 174 (3), 1635–1659.

Morata, G., Ripoll, P., 1975. Minutes: mutants of *Drosophila* autonomously affecting cell division rate. Dev. Biol. 42, 211–221.

Moreno, E., Basler, K., Morata, G., 2002. Cells compete for decapentaplegic survival factor to prevent apoptosis in *Drosophila* wing development. Nature 416, 755–759.

Moreno, E., Basler, K., 2004. DMyc transforms cells into super-competitors. Cell 117 (1), 117–129.

Muller, H., Fogeron, M.L., Lehmann, V., Lehrach, H., Lange, B.M., 2006. A centrosome-independent role for gamma-TuRC proteins in the spindle assembly checkpoint. Science 314, 654–657.

Nagel, A.C., Maier, D., Preiss, A., 2002. Green fluorescent protein as a convenient and versatile marker for studies on functional genomics in *Drosophila*. Dev. Genes Evol. 212 (2), 93–98.

Ollmann, M., Young, L.M., Di Como, C.J., Karim, F., Belvin, M., Robertson, S., Whittaker, K., Demsky, M., Fisher, W.W., Buchman, A., Duyk, G., Friedman, L., Prives, C., Kopczynski, C., 2000. *Drosophila* p53 is a structural and functional homolog of the tumor suppressor p53. Cell 101 (1), 91–101.

Oskarsson, T., Essers, M.A., Dubois, N., Offner, S., Dubey, C., Roger, C., Metzger, D., Chambon, P., Hummler, E., Beard, P., Trumpp, A., 2006. Skin epidermis lacking the c-Myc gene is resistant to Ras-driven tumorigenesis but can reacquire sensitivity upon additional loss of the p21Cip1 gene. Genes Dev. 20 (15), 2024–2029.

Pan, D., 2007. Hippo signalling in organ size. Genes Dev. 21, 886–897.

Pellock, B.J., Buff, E., White, K., Hariharan, I.K., 2007. The *Drosophila* tumor suppressors Expanded and Merlin differentially regulate cell cycle exit, apoptosis, and Wingless signaling. Dev. Biol. 304 (1), 102–115.

Price, D., Rabinovitch, S., O'Farrell, P.H., Campbell, S.D., 2000. Drosophila wee1 has an essential role in the nuclear divisions of early embryogenesis. Genetics 155, 159–166.

Price, D.M., Jin, Z., Rabinovitch, S., Campbell, S.D., 2002. Ectopic expression of the *Drosophila* Cdk1 inhibitory kinases, Wee1 and Myt1, interferes with the second mitotic wave and disrupts pattern formation during eye development. Genetics 161 (2), 721–731.

Prober, D.A., Edgar, B.A., 2000. Ras1 promotes cellular growth in the *Drosophila* wing. Cell 100 (4), 435–446.

Royzman, I., Whittaker, A.J., Orr-Weaver, T.L., 1997. Mutations in *Drosophila* DP and E2F distinguish G1-S progression from an associated transcriptional program. Genes Dev. 11 (15), 1999–2011.

Ryoo, H.D., Gorenc, T., Steller, H., 2004. Apoptotic cells can induce compensatory cell proliferation through the JNK and the Wingless signaling pathways. Dev. Cell 7 (4), 491–501.

Secombe, J., Pispa, J., Saint, R., Richardson, H., 1998. Analysis of a *Drosophila* cyclin E hypomorphic mutation suggests a novel role for cyclin E in cell proliferation control during eye imaginal disc development. Genetics 149 (4), 1867–1882.

Spradling, A.C., Rubin, G.M., 1982. Transposition of cloned P elements into *Drosophila* germ line chromosomes. Science 218, 341–347.

Stumpff, J., Kellogg, D.R., Krohne, K.A., Su, T.T., 2005. *Drosophila* Wee1 interacts with members of the gammaTURC and is required for proper mitotic-spindle morphogenesis and positioning. Curr. Biol. 15 (17), 1525–1534.

Sumara, I., Gimenez-Abian, J.F., Gerlich, D., Hirota, T., Kraft, C., de la Torre, C., Ellenberg, J., Peters, J.M., 2004. Roles of polo-like kinase 1 in the assembly of functional mitotic spindles. Curr. Biol. 14 (19), 1712–1722.

Vachon, G., Cohen, B., Pfeifle, C., McGuffin, M.E., Botas, J., Cohen, S.M., 1992. Homeotic genes of the Bithorax complex repress limb development in the abdomen of the *Drosophila* embryo through the target gene Distal-less. Cell 71 (3), 437–450.

Vidwans, S.J., Wong, M.L., O'Farrell, P.H., 2003. Anomalous centriole configurations are detected in *Drosophila* wing disc cells upon Cdk1 inactivation. J. Cell Sci. 116, 137–143.

Weigmann, K., Cohen, S.M., Lehner, C.F., 1997. Cell cycle progression, growth and patterning in imaginal discs despite inhibition of cell division after inactivation of *Drosophila* Cdc2 kinase. Development 124 (18), 3555–3563.

Wu, S., Huang, J., Dong, J., Pan, D., 2003. Hippo encodes a Ste-20 family protein kinase that restricts cell proliferation and promotes apoptosis in conjunction with salvador and warts. Cell 114 (4), 445–456.